Opt Quant Electron (2016) 48:280
DOI 10.1007/s11082-016-0562-6

A comparative study of different metal and prism in the surface plasmon resonance biosensor having MoS_2-graphene

J. B. Maurya[1] · **Y. K. Prajapati**[1]

Received: 16 December 2015 / Accepted: 8 April 2016 / Published online: 13 April 2016

Abstract In the present study, the optimum range of prism refractive index and better surface plasmons active metals for biosensing application are obtained on the basis of performance of the proposed SPR sensor. Proposed sensor utilizes the properties of graphene and MoS_2 such as; mechanically strong, atomically thin and chemically inert coating for the protection against oxidation of SPs active metal. It is observed that the prism having moderate refractive index should be preferred and sensor having silver (Ag) has minimum full width at half maximum whereas copper (Cu) has maximum shift in resonance angle. Hence, Ag can be used for high quality and resolution whereas Cu for good sensitivity, which are protected from oxidation with the help of two dimensional MoS_2 or graphene, or graphene over MoS_2.

Keywords Surface plasmon resonance · Sensor · Pseudomonas · ssDNA

1 Introduction

"In the conventional SPR sensor, the SPs active metals are; gold (Au), silver (Ag), copper (Cu), aluminium (Al), sodium (Na), and indium (In) (Raether 1988). The 'Na' is a reactive in nature, 'In' is very expensive, whereas 'Ag,' 'Cu,' and 'Al' are susceptible to oxidation, in contrast 'Au' is resistant to oxidation and corrosion in different environments and most practical in nature. Hence, 'Au' is the best choice as an SPs active metal in the conventional SPR sensor. However, bare 'Au' surface is not suited well for the biosensor because

✉ Y. K. Prajapati
yogendrapra@gmail.com

J. B. Maurya
jitendra.maurya06@gmail.com

[1] Electronics and Communication Engineering Department, Motilal Nehru National Institute of Technology Allahabad, Allahabad, Uttar Pradesh 211004, India

of its poor absorbance nature against biomolecules (Wu et al. 2010). Hence, the traditional biosensors are not capable of sensing ssDNA virus and Pseudomons-like bacteria due to the poor attachment of these biomolecules on the bare metal surface. To sensing DNA, chemicals, proteins, organic molecules and inorganic ions, colorimetric sensors based on different plasmonic nanomaterials of different shapes could be a better option (Polavarapu et al. 2014; Shiohara et al. 2014). But these sensors suffers from inhomogeneity in the color distribution and the coffee ring effect in the detection zones due to which making decision of the final color by naked eye is a challenging factor (Abe et al. 2008). In addition, colorimetric sensors are affected by the background color of the paper or the sample (Yetisen 2015). Moreover, the functionalize plasmonic nanoparticles such as gold nanoparticles (AuNP), ligand-stabilized AuNPs, for colorimetric detection suffers from several drawbacks; separation of ligands for functionalizing AuNPs e.g. DNA could be costly, covalent conjugation of bioactive ligands onto the surface of AuNPs may partially sacrifice their reactivities. These drawbacks can be overcome by unmodified AuNPs but there are still two drawbacks; identification without the instruments i.e. by naked eye can at best provide a semi-quantitative result, unmodified AuNPs are less tolerant to interference than functionalized AuNPs (Sha et al. 2011).

Hence, in order to detect ssDNA virus and Pseudomons-like bacteria the application of optical properties of not only the individual MoS_2 or graphene layers but also the combined heterostructure of MoS_2-graphene (MoS_2 over graphene layer) in the SPR sensor are aimed to study. Where, the graphene takes the advantage of attaching these biomolecule with the help of π-stacking property (McGaughey et al. 1998) between graphene and carbon rings presented in the biomolecules. Whereas, single layer MoS_2 nanosheet exhibits high fluorescence quenching ability and affinity towards ssDNA. Therefore, MoS_2 is able to adsorb the dye-labeled ssDNA probe via the van der Waals force between nucleobases and the basal plane of MoS_2 (Zhu et al. 2013). Apart from these unique attachment properties, graphene as well as MoS_2 has large surface to volume ratio which is suitable for making contact with analytes (Novoselov et al. 2004; Mak et al. 2010). Furthermore, the performance of the sensor can be enhanced by using graphene along with MoS_2 rather using only graphene or only MoS_2. The monolayer MoS_2 has much higher optical absorption coefficiency ($\sim$5 %) (Lopez-Sanchez et al. 2013) than that of the graphene layer ($\sim$2.3 %) (Maurya et al. 2015). The electron energy loss of MoS_2 layer is comparable to that of graphene and this will allow a successful ($\sim$100 %) of light energy transfer to the graphene–MoS_2 coated sensing substrate. Such process will lead to a significant enhancement of SPR signals (Maurya et al. 2015a, b, 2016). Hence, in place of using bare metal surface it is beneficial to use metal surface covered with nanolayers such as; MoS_2 and graphene. In 2010, Song et al. (2010) presented a highly conductive material with excellent adsorption properties for high-resolution bio/nano detection and identification using graphene-on-gold. The key reason behind this unique property is that graphene can stably (Tang et al. 2010) adsorb carbon-based rings, which are widely present in biomolecules, due to π-stacking interactions (McGaughey et al. 1998) while pertaining the excellent conductivity of gold as substrate. By using this concept, Wu et al. (2010) and Verma et al. (2014) have presented an SPR sensor based on graphene-on-gold for enhancing the performance of sensor. Because of the high charge carrier mobility (10^6 cm^2 V^{-1} s^{-1}), when graphene is deposited on metallic thin films, strong coupling is induced at the metal-graphene interface and due to which a large electric field enhancement takes place (Elias et al. 2011). In contrast to gold, silver has sharper SPR curve (Ong et al. 2006) which is always required for a good sensor but silver is highly susceptible to oxidation, and the increased thickness of silver oxide makes SPR curve broader. The silver may be a better

choice rather gold if somehow it could be protected from oxidation. In this regards, it is noticed that graphene is impermeable to gases as small as Helium (He) (Bunch et al. 2008) because electron density of hexagonal rings is substantial enough to prevent atoms and molecules (e.g. Oxygen gases) from passing through the ring structure (Jiang et al. 2009). Using this concept in 2011, Choi et al. (2011) have presented a sensor having silver as a SPs active metal and the oxidation of which is protect by graphene as a result of which the sensitivity increased three times when compared with the conventional gold substrate. Copper and Aluminium get oxidized similar to silver with the difference of having different thickness of oxidized layer. In 2006, Mitsushio et al. 2006 showed that the thickness of oxide layers for silver is 0.3 nm whereas those for the copper and aluminium are 2 nm. And in 2014, Kravets et al. 2014 have successfully used graphene as protective layer against oxidation of copper and identified that graphene can employed also for other metals such as silver and aluminium.

Hence, for the first time as per the best of our knowledge, theoretical along with numerical analysis of SPR biosensor utilizing MoS_2-graphene as protection layer against oxidation of SPs active metal layer is proposed. The paper is organized as follows. In the section II of this paper the theoretical modeling and performance parameter with mathematical expression is presented. In the section III the results are discussed in detail. Finally, the paper ends with the conclusion and necessary references regarding to the proposed work are given."

2 Design consideration and theoretical model

The proposed sensor structure is shown in Fig. 1. The wavelength under consideration is 632.8 nm. At this wavelength the refractive index (RI) of the prisms BK7, SF11, and chalcogenide (2S2G) are 1.5151, 1.7786 (Maurya et al. 2015), and 2.3581 (Verma et al. 2016) respectively. The RI of the metals 'Au', 'Ag', 'Cu', and 'Al' are $0.14330 + 3.6080i$, $0.051255 + 4.3165i$, $0.10926 + 3.5802i$, and $1.1528 + 6.6898i$ (McPeak et al. 2015) respectively. The RI of the nanolayers MoS_2 and graphene are $5.9 + 0.8i$, $3 + 1.1487i$ (Maurya et al. 2015) respectively. The RI of the cover layer i.e. the top most layer is 1.332 (Maurya et al. 2015). The thicknesses of the metal layers are optimized and it

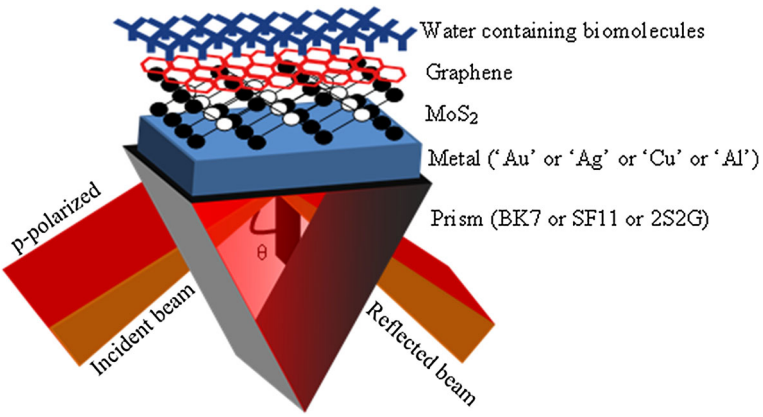

Fig. 1 Schematic diagram of the proposed surface plasmon resonance biosensor strucrure

is seen (shown later in this paper) that the optimized thickness of the metal layers for 'Au', 'Ag', 'Cu', and 'Al' are 49 nm, 55 nm, 53 nm, and 14 nm. The thicknesses of the nanolayers MoS_2 and graphene are L × 0.66 nm and G × 0.34 nm respectively where 'L' and 'G' are the number of layers of the MoS_2 and graphene.

The transfer matrix method (TMM) and Fresnel equations based on N-layer model is employed for the systematic investigation of the reflectivity in the proposed SPR sensing system (Maurya et al. 2015).

The plot of reflectivity versus incident angle (θ_i) is called SPR curve. The incident angle corresponding to the minimum value of the reflectivity is known as resonance angle (θ_{res}). The resonance angle changes with the refractive index change (Δn_s) of the sensing medium due to the attachment of the targeted biomolecules. The shifting of the resonance angle is just because of the wave vector matching between the incident light (k_x) and the surface plasmon wave (k_{SP}) which are given as follows;

$$k_x = k_0 n_p \sin\theta_{res}, \quad \text{and} \quad k_{SP} = Re\left[k_0\left(\frac{\varepsilon_{mmg} n_s^2}{\varepsilon_{mmg} + n_s^2}\right)^{1/2}\right] \tag{1}$$

where k_0 is the wave vector of the incident light in free space, n_p and n_s are the RI of the prism and sensing medium, ε_{mmg} is the dielectric constant of the MoS_2-graphene enhanced metallic thin layer. It is obvious from Eq. (1) that at fixed operating wavelength the value of the k_{SP} can be varied if the RI of the sensing medium changes, hence in order to obtain the resonance condition ($k_x = k_{SP}$) the resonance angle must change. Consequently, it can be said that by measuring the shift in the resonance angle ($\Delta\theta_{res}$) the amount of absorbed biomolecules (Δn_s) can be measured. The sensitivity to the RI change (S_{RI}) of the sensor, one of the performance parameter, can be defined as the ratio of the shift in resonance angle to the change in the RI of the sensing medium;

$$S_{RI} = \frac{\Delta\theta_{res}}{\Delta n_s} \tag{2}$$

The adsorption efficiency (E) of the target biomolecules on the biomolecular recognition element can be defined as;

$$E = \frac{\Delta n_s}{\Delta M} \tag{3}$$

The E represents the percent of biomolecules in the water that can be adsorbed and converted into the change in the RI of the sensing medium.

Hence, the overall sensitivity of the sensor (S) is defined as the ratio of the shift in the resonance angle ($\Delta\theta_{res}$) to the change in the moles of biomolecules (ΔM) (Wu et al. 2010);

$$S = \frac{\Delta\theta_{res}}{\Delta M} = \frac{\Delta\theta_{res}}{\Delta n_s} \cdot \frac{\Delta n_s}{\Delta M} = S_{RI} \cdot E \tag{4}$$

It is observed from Eq. (4) that sensitivity is directly proportional to the $\Delta\theta_{res}$ due to which the nature of the plots of sensitivity and $\Delta\theta_{res}$ will be same. Hence, only $\Delta\theta_{res}$ is calculated in this paper for the sake of increased calculation.

Another performance parameter is fullwidth at half maximum (FWHM) which measures the broadness of the SPR curve. For better high resolution (detection accuracy) and high quality the FWHM should be as low as possible (Maurya et al. 2015).

3 Results and discussion

After defining the refractive indices of all the layers, it is required to optimize the thickness of constituting layers in order to get better performance of the sensor. Hence, for the optimization of metal layers, in Fig. 2, the sensitivity and minimum reflectance (Rmin) is plotted in accordance with the thickness of metal layers 'Au', 'Ag', 'Cu', and 'Al'. For better performance of the sensor the high sensitivity along with minimum Rmin is desired. Because we are interested in the maximum value of the sensitivity, the undesired sudden dip in the sensitivity plots will not affect the choice of optimized thickness. The maximum sensitivity and minimum Rmin are respectively for 'Au' 73.04 (100 nm) and 2.14×10^{-4} (49 nm), for 'Ag' 64.35 (28 nm) and 0.22×10^{-4} (55 nm), for 'Cu' 73.46 (100 nm) and 0.11×10^{-4} (53 nm), and 'Al' 62.26 (8 nm) and 8.28×10^{-4} (14 nm). One can easily observe from the plots that the Rmin at maximum sensitivity is very high which is undesired. But fortunately the sensitivity at minimum Rmin has value approximately equal to the maximum sensitivity which makes it very easy to choose the thickness of metal layer corresponding to the minimum Rmin. Hence the optimized thickness for 'Au' is 49 nm, for 'Ag' is 55 nm, for 'Cu' is 53 nm, and for 'Al' is 14 nm.

In Fig. 3, the sensitivity, Rmin, and FWHM are plotted in accordance with the prism RI at optimized gold layer thickness. The sensitivity axis is the left black vertical axis, whereas Rmin axis is the right red vertical axis, and FWHM axis is the right blue vertical axis. The curves below 1.41 RI of the prism are abrupt in nature because of non-existence of the solid material for the prism. The Rmin is approximately zero after 1.41 RI of the prism hence it will not play crucial role in deciding the approximate RI of prism. One can notice from this figure that the sensitivity and FWHM decreases with increasing the RI of the prism. Hence in order to fulfill the demand of high sensitivity and low FWHM, the RI of the prism should be in the moderate range. If we consider the three well-known prisms i.e. BK7, SF11 and 2S2G the RI of which at 632.8 nm wavelength are 1.5151, 1.7786, and

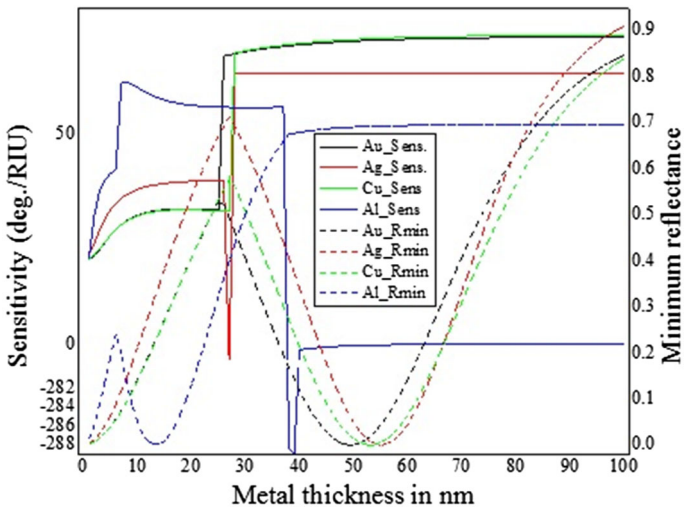

Fig. 2 Thickness optimization of gold (*black*), silver (*red*), copper (*green*), and aluminium (*blue*) layers with respect to sensitivity (*solid curves*) and minimum reflectance (*dashed curves*), at SF11 prism. (Color figure online)

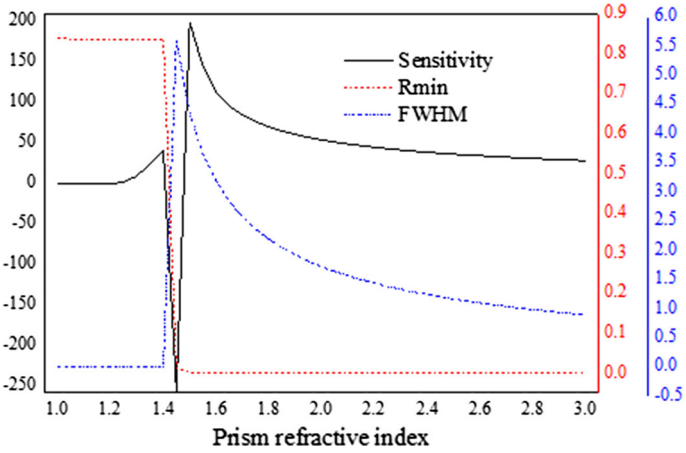

Fig. 3 The variation of sensitivity (*black solid curve*), minimum reflectance (*red dashed curve*), FWHM (*blue dash-dot curve*) in accordance with the prism refractive index, at optimized gold layer thickness. (Color figure online)

2.3581 respectively, SF11 is the better choice for better performance of the sensor. For having more clear observation, in Fig. 4 the SPR curves for these three prisms are plotted at 1.332 and 1.40 RI of the sensing medium at optimized gold layer thickness which shows the shift in resonance angle, Rmin and FWHM (as shown in Table 1). From Table 1 it can be clearly observed that SF11 prism has moderate shift in resonance angle hence according to Eq. (4) the sensitivity will be moderate, and also the FWHM is moderate. One can choose BK7 prism for higher sensitivity but for this the resolution (inversely proportional to the FWHM) will be poor, or 2S2G prism for higher resolution but for this the sensitivity will be poor. Hence, in this paper the SF11 is chosen for further plots.

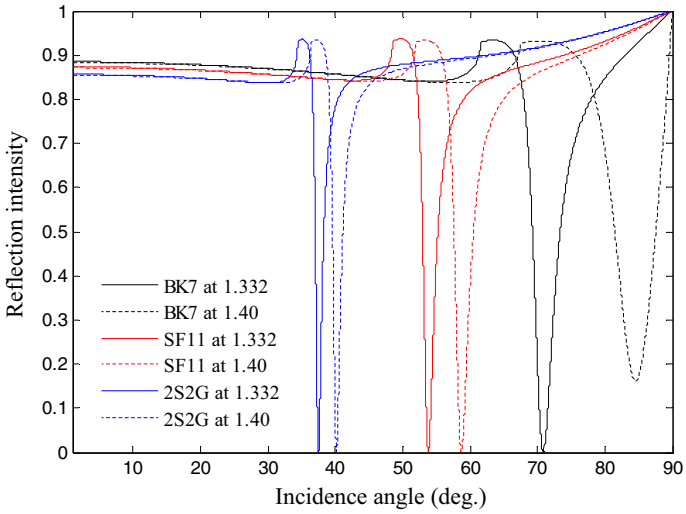

Fig. 4 The variation of reflection intensity in accordance of incidence angle for BK7 (*black*), SF11 (*red*), and 2S2G (*blue*) prism, at optimized gold layer thickness, for sensing layer refractive index 1.332 (*solid curves*) and 1.40 (*dashed curves*). (Color figure online)

Table 1 The resonance angle (θ_{res}), shift in resonance angle ($\Delta\theta_{res}$), minimum reflectance (*Rmin*), and FWHM of the SPR *curves* for BK7, SF11, and 2S2G prisms at optimized gold layer thickness

Prism	θ_{res}		$\Delta\theta_{res}$	*Rmin* ($\times 10^{-4}$)		FWHM	
	$n_s = 1.332$	$n_s = 1.40$	$\Delta n_s = 0.068$	$n_s = 1.332$	$n_s = 1.40$	$n_s = 1.332$	$n_s = 1.40$
BK7	70.86	84.56	13.70	4.57	1615	4.10	5.99
SF11	53.80	58.71	4.90	2.14	0.29	2.25	2.90
2S2G	37.50	40.17	2.67	1.68	0.082	1.27	1.53

In Fig. 5, the SPR curves are plotted for different metals under consideration at 1.332 and 1.40 RI of the sensing medium showing the shift in resonance angle, Rmin and FWHM (as shown in Table 2). It is clearly observed from this plot that the SPR curves for all the metals have expected shape. Form Table 2 it is observed that $\Delta\theta_{res}$ for 'Au' is high but the FWHM is also very high which is not desired, whereas for the 'Al' the $\Delta\theta_{res}$ is lowest and FWHM is very high hence this will give the worst performance. The $\Delta\theta_{res}$ for the 'Cu' is highest and also have low FWHM which is always desired hence 'Cu' can be chosen for the better performance than 'Au' and 'Al'. It worth noting here that the 'Ag' has $\Delta\theta_{res}$ approximately equal to the 'Cu' but the FWHM for the 'Ag' is very low giving the highest resolution while maintaining the sensitivity. Hence, 'Ag' is the best choice as SPs active metal and 'Cu' can be given as the second choice. Hence, in this paper 'Ag' and 'Cu' will be considered for further investigation.

Although 'Ag' and 'Cu' gives the high sensitivity with high resolution but these SPs active metals suffer from the highly susceptible nature towards oxidation. And the situation becomes worst when the thickness of their oxide is increased which rises the broadening of

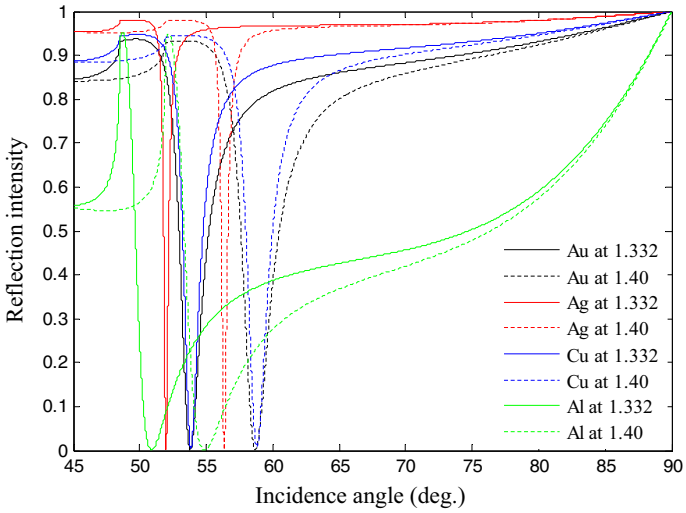

Fig. 5 The variation of reflection intensity in accordance of incidence angle for gold (*black*), silver (*red*), copper (*blue*), and aluminium (*green*) layers, at SF11 prism, for sensing layer refractive index 1.332 (*solid curves*) and 1.40 (*dashed curves*). (Color figure online)

Table 2 The resonance angle (θ_{res}), shift in resonance angle ($\Delta\theta_{res}$), minimum reflectance (*Rmin*), and FWHM of the SPR curves for 'Au', 'Ag', 'Cu', 'Al' at SF11 prism

Metal	θ_{res}		$\Delta\theta_{res}$	*Rmin* ($\times 10^{-4}$)		FWHM	
	$n_s = 1.332$	$n_s = 1.40$	$\Delta n_s = 0.068$	$n_s = 1.332$	$n_s = 1.40$	$n_s = 1.332$	$n_s = 1.40$
Au	53.80	58.70	4.90	2.14	0.29	2.25	2.90
Ag	51.98	56.35	4.38	0.22	0.35	0.39	0.50
Cu	53.85	58.81	4.96	51.98	75.59	1.55	2.01
Al	50.89	54.87	3.98	10.89	0.55	20.74	22.98

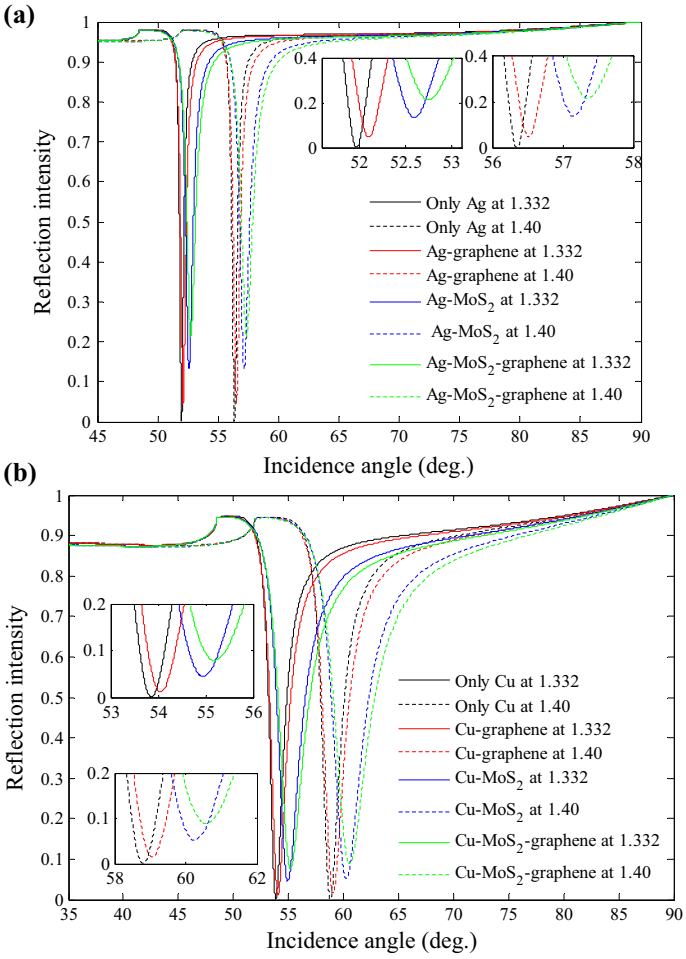

Fig. 6 The variation of reflection intensity in accordance of incidence angle for sensor having only metal (*black*), metal-graphene (*red*), metal-MoS_2 (*blue*), and metal-MoS_2-graphene (*green*) layers at optimized metal layer thickness and monolayer graphene and MoS_2, for sensing layer refractive index 1.332 (*solid curves*) and 1.40 (*dashed curves*); **a** metal is silver, **b** metal is copper. (Color figure online)

the SPR curve. Hence as it is seen that the 'Ag' and 'Cu' may be the better choice rather 'Au' if somehow it could be protected from oxidation. Hence in order to protect these metals from the oxidation, MoS_2 and graphene are chosen as protective layer because they are impermeable to gases as small as Helium (Bunch et al. 2008). The electron density of the monolayer MoS_2 and graphene is substantial enough to prevent atoms and molecules (e.g. Oxygen gases) from passing through their structure (Jiang et al. 2009).

Although MoS_2 and graphene are able to protect the 'Ag' and 'Cu' from oxidation but it is necessary to see the effect of adding these layers over the 'Ag' and 'Cu' on the performance of the sensor. Hence in order to see these effects, comparative SPR plots of the sensor having only metal layer, metal-graphene layer, metal-MoS_2 layer, and metal-MoS_2-graphene layer are plotted in Fig. 6. In Fig. 6a the metal layer is 'Ag' whereas in Fig. 6b it is 'Cu'. The Fig. 6a, b show the shift in resonance angle, Rmin and FWHM (as shown in Table 3). For more clear observations of the Rmin the SPR curves at 1.332 and 1.40 are shown in inset. From Table 3 it can be clearly observed that the decreasing order of $\Delta\theta_{res}$ is; metal-MoS_2-graphene > metal-MoS_2 > metal-graphene > only metal and the same order is for their thickness. It means as the thickness of the nanolayers increases the absorption increases which rises the $\Delta\theta_{res}$ (Maurya et al. 2015). From this table it is also observed as the nanolayers MoS_2 or graphene or both are added over the metal layer the Rmin and FWHM increases. Because of the addition of the nanolayers over metal layers SPs damping occurs which makes the SPR curve shallower and broader (Pockrand 1978). Shallowing of the SPR curves results in higher Rmin and broadening of the SPR curves results in larger FWHM.

Now, for the verification of the generation of SPs at MoS_2-graphene enhanced metal-dielectric interfaces of the sensor, the TM field intensity are plotted in accordance with the distance normal to the interface for 'Ag' and 'Au' in Fig. 7a, b respectively. Inset is shown for clear observation of the decay rate of the TM field inside Mos_2 and graphene layers. At the resonance angle the intensity of the EM field attains its maximum value. Since the most of the EM field at the resonance condition is used in the generation of the SPs, the

Table 3 The resonance angle (θ_{res}), shift in resonance angle ($\Delta\theta_{res}$), minimum reflectance (*Rmin*), and FWHM of the SPR curves for only metal, metal-graphene, metal-MoS_2, and metal-MoS_2-graphene at SF11 prism; the metal is either 'Ag' or 'Cu'

Prism	θ_{res}		$\Delta\theta_{res}$	*Rmin* ($\times 10^{-4}$)		FWHM	
	$n_s = 1.332$	$n_s = 1.40$	$\Delta n_s = 0.068$	$n_s = 1.332$	$n_s = 1.40$	$n_s = 1.332$	$n_s = 1.40$
Only Ag	51.98	56.35	4.38	0.22	0.35	0.39	0.50
Ag-graphene	52.11	56.52	4.41	463.94	478.5	0.49	0.64
Ag-MoS_2	52.60	57.16	4.56	1333.29	1333.53	0.64	0.85
Ag-MoS_2-graphene	52.75	57.36	4.61	21,237.00	2140.32	0.70	0.92
Only Cu	53.86	58.81	4.95	0.11	1.04	1.67	2.17
Cu-graphene	54.06	59.07	5.01	110.89	147.69	1.93	2.51
Cu-MoS_2	54.95	60.26	5.31	445.87	520.33	2.63	3.42
Cu-MoS_2-graphene	55.19	60.58	5.38	785.98	891.48	2.89	3.76

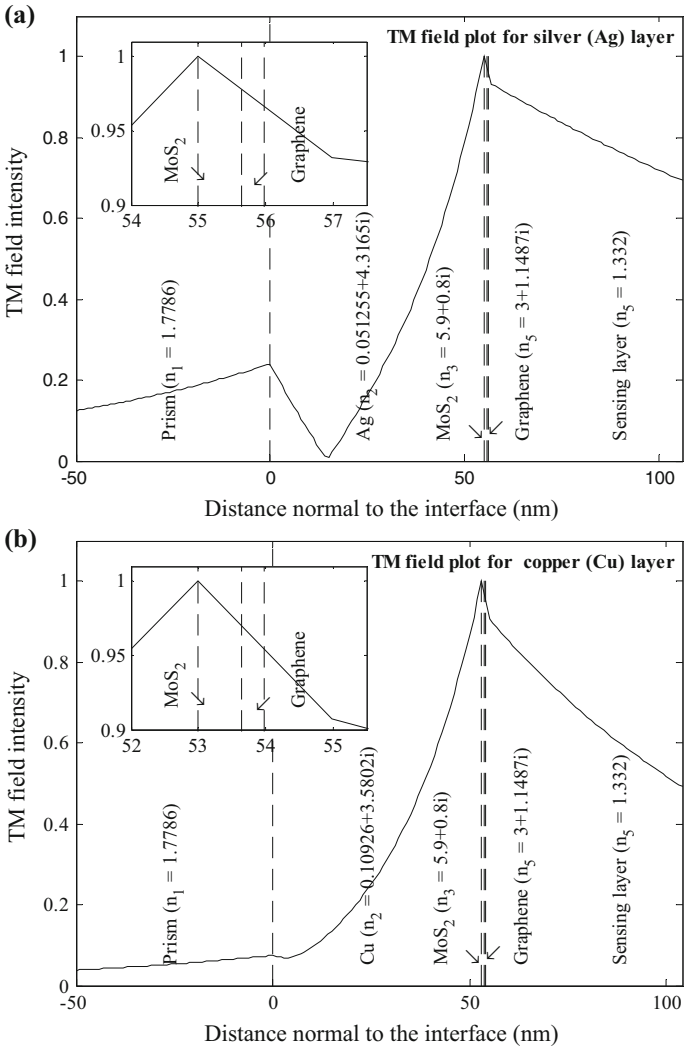

Fig. 7 The transverse magnetic field plot in accordance with the distance normal to the interface of layers, at SF11 prism, for optimized thickness of metal layer and monolayer MoS_2 and graphene, at sensing layer refractive index 1.332; **a** metal layer is silver, **b** metal layer is copper

reflection intensity (R) attains its minimum value (Rmin). In the Fig. 7a, b the TM field is maximum at the metal-MoS_2 interface giving rise to the maximum generation of the SPs. This maximum field is suddenly decreased by the MoS_2 and graphene layer and then decays continuously in the sensing medium. Hence in order to sense the biomolecules the intensity of the TM field should decrease exponentially, which is also termed as the evanescent field, in the sensing medium and tends to infinite depth. One can also say that by increasing the evanescent depth in the sensing medium, the interaction volume of evanescent field with the biomolecules is increased which in turn maximize the sensitivity (Shalabney and Abdulhalim 2010).

4 Conclusion

For the proposed sensor having MoS_2 and graphene the RI of the prism should be high for lower FWHM whereas it should be low for higher sensitivity. It is observed that the Ag has minimum FWHM whereas Cu has maximum shift in resonance angle. Hence Ag can be used for high quality and resolution whereas Cu for good sensitivity. By the addition of MoS_2 and graphene sensitivity is improved due to increased absorption and FWHM is increased due to SPs damping. Hence, it is believed that the sensor having MoS_2 and graphene can have potential use in the detection of ssDNA and Pseudomonas, whose detection are not possible by the conventional sensor due to poor attachment of these biomolecules on the bare metal surfaces.

References

Abe, K., Suzuki, K., Citterio, D.: Inkjet-printed microfluidic multianalyte chemical sensing paper. Anal. Chem. **80**(18), 6928–6934 (2008)

Bunch, J.S., Verbridge, S.S., Alden, J.S., van der Zande, A.M., Parpia, J.M., Craighead, H.G., McEuen, P.L.: Impermeable atomic membranes from graphene sheets. Nano Lett. **8**(8), 2458–2462 (2008)

Choi, S.H., Kim, Y.L., Byun, K.M.: Graphene-on-silver substrates for sensitive surface plasmon resonance imaging biosensors. OSA Opt. Express **19**(2), 458–466 (2011)

Elias, D.C., Gorbachev, R.V., Mayorov, A.S., Morozov, S.V., Zhukov, A.A., Blake, P., Ponomarenko, L.A., Grigorieva, I.V., Novoselov, K.S., Guinea, F., Geim, A.K.: Dirac cones reshaped by interaction effects in suspended graphene. Nat. Phys. **7**, 701–704 (2011)

Jiang, D.E., Cooper, V.R., Dai, S.: Porous graphene as the ultimate membrane for gas separation. Nano Lett. **9**(12), 4019–4024 (2009)

Kravets, V. G., Jalil, R., Kim, Y. J., Ansell, D., Aznakayeva, D. E., Thackray, B., Britnell, L., Belle, B. D., Withers, F., Radko, I. P., Han, Z., Bozhevolnyi, S. I., Novoselov, K. S., Geim, A. K., Grigorenko, A. N.: Graphene-protected copper and silver plasmonics. Sci. Rep. **4**, 5517 (2014)

Lopez-Sanchez, O., Lembke, D., Kayci, M., Radenovic, A., Kis, A.: Ultrasensitive photodetectors based on monolayer MoS_2. Nat. Nanotechnol. **8**(7), 497–501 (2013)

Mak, K.F., Lee, C., Hone, J., Shan, J., Heinz, T.F.: Atomically thin MoS_2: a new direct-gap semiconductor. Phys. Rev. Lett. **105**, 136805 (2010)

Maurya, J.B., Prajapati, Y.K., Singh, V., Saini, J.P.: Sensitivity enhancement of surface plasmon resonance sensor based on graphene–MoS_2 hybrid structure with TiO2–SiO2 composite layer. Appl. Phys. A **121**(2), 525–5333 (2015a)

Maurya, J.B., Prajapati, Y.K., Singh, V., Saini, J.P., Tripathi, R.: Performance of graphene–MoS2 based surface plasmon resonance sensor using Silicon layer. Opt. Quant. Electron. **47**(11), 3599–3611 (2015b)

Maurya, J.B., Prajapati, Y.K., Singh, V., Saini, J.P., Tripathi, R.: Improved performance of the surface plasmon resonance biosensor based on graphene or MoS_2 using silicon. Opt. Commun. **359**, 426–434 (2016)

McGaughey, G.B., Gagné, M., Rappé, A.K.: π-Stacking interactions. Alive and well in proteins. J. Biol. Chem. **273**(25), 15458–15463 (1998)

McPeak, K.M., Jayanti, S.V., Kress, S.J.P., Meyer, S., Iotti, S., Rossinelli, A., Norris, D.J.: Plasmonic films can easily be better: rules and recipes. ACS Photonics **2**, 326–333 (2015)

Mitsushio, M., Miyashita, K., Higo, M.: Sensor properties and surface characterization of the metal-deposited SPR optical fiber sensors with Au, Ag, Cu, and Al. Sens. Actuators A **125**(2), 296–303 (2006)

Novoselov, K.S., Geim, A.K., Morozov, S.V., Jiang, D., Zhang, Y., Dubonos, S.V., Grigorieva, I.V., Firsov, A.A.: Electric field effect in atomically thin carbon films. Science **306**(5696), 666–669 (2004)

Ong, B.H., Yuan, X., Tjin, S.C., Zhang, J., Ng, H.M.: Optimised film thickness for maximum evanescent field enhancement of a bimetallic film surface plasmon resonance biosensor. Sens. Actuators B Chem. **114**(2), 1028–1034 (2006)

Pockrand, I.: Surface plasma oscillations at silver surfaces with thin transparent and absorbing coatings. Surf. Sci. **72**, 577–588 (1978)

Polavarapu, L., Pérez-Juste, J., Xu, Q.H., Liz-Marzan, L.M.: Optical sensing of biological, chemical and ionic species through aggregation of plasmonic nanoparticles. J. Mater. Chem. C **2**, 7460–7476 (2014)

Raether, H.: Surface Plasmons on Smooth and Rough Surfaces and on Gratings. Springer, Berlin (1988)

Sha, H.E., DingBin, L., Zhuo, W., KaiYong, C., XingYu, J.: Utilization of unmodified gold nanoparticles in colorimetric detection. Sci. China Phys. Mech. Astron. **54**(10), 1757–1765 (2011)

Shalabney, A., Abdulhalim, I.: Electromagnetic fields distribution in multilayer thin film structures and the origin of sensitivity enhancement in surface plasmon resonance sensors. Sens. Actuators A **159**(1), 24–32 (2010)

Shiohara, A., Langer, J., Polavarapua, L., Liz-Marzan, L.M.: abSolution processed polydimethylsiloxane/gold nanostar flexible substrates for plasmonic sensing. Nanoscale **6**, 9817–9823 (2014)

Song, B., Li, D., Qi, W.P., Elstner, M., Fan, C.H., Fang, H.P.: Graphene on Au (111): a highly conductive material with excellent adsorption properties for high-resolution bio/nanodetection and identification. ChemPhysChem **11**(3), 585–589 (2010)

Tang, Z., Wu, H., Cort, J.R., Buchko, G.W., Zhang, Y., Shao, Y., Aksay, I.A., Liu, J., Lin, Y.: Constraint of DNA on functionalized graphene improves its biostability and specificity. Small **6**(11), 1205–1209 (2010)

Verma, A., Prakash, A., Tripathi, R.: Performance analysis of graphene based surface plasmon resonance biosensors for detection of pseudomonas-like bacteria. Opt. Quant. Electron. **47**(5), 1197–1205 (2014)

Verma, A., Prakash, A., Tripathi, R.: Sensitivity improvement of graphene based surface plasmon resonance biosensors with chaclogenide prism. Optik-Int. J. Light Electron Opt. **127**(4), 1787–1791 (2016)

Wu, L., Chu, H.S., Koh, W.S., Li, E.P.: Highly sensitive graphene biosensors based on surface plasmon resonance. OSA Opt. Express **18**(14), 14395–14440 (2010)

Yetisen, A.K.: Fundamentals of Holographic Sensing. *Holographic Sensors*. Springer International Publishing, Berlin (2015)

Zhu, C., Zeng, Z., Li, H., Li, F., Fan, C., Zhang, H.: Single-layer MoS_2-based nanoprobes for homogeneous detection of biomolecules. J. Am. Chem. Soc. **135**, 5998–6001 (2013)